

Quantitative analysis of nanoscale switching in $\text{SrBi}_2\text{Ta}_2\text{O}_9$ thin films by piezoresponse force microscopy

Sergei V. Kalinin^{a)}

Condensed Matter Sciences Division, Oak Ridge National Laboratory, Oak Ridge, Tennessee 37831

Alexei Gruverman

Department of Materials Science and Engineering, North Carolina State University, Raleigh, North Carolina 27695

Dawn A. Bonnell

Department of Materials Science and Engineering, The University of Pennsylvania, Philadelphia, Pennsylvania 19104

(Received 6 January 2004; accepted 29 May 2004)

Local switching properties in $\text{SrBi}_2\text{Ta}_2\text{O}_9$ thin films have been studied by spatially resolved piezoresponse force microscopy (PFM) and spectroscopy. Variations in PFM contrast of individual grains due to their random crystallographic orientation are consistent with the grain switching behavior examined via vertical and lateral hysteresis loops. Theoretical description of vertical hysteresis loop shape obtained in the point-charge approximation is shown to be in good agreement with the experimental data. Dependence of the hysteresis loop parameters on the grain crystallographic orientation is analyzed. It has been found that grain deviation from the ideal (010) orientation when the polar axis is normal to the film plane results in the decrease of the PFM signal and increase of the coercive voltage in agreement with theoretical predictions. © 2004 American Institute of Physics. [DOI: 10.1063/1.1775881]

Progress in electronic devices based on ferroelectric heterostructures requires an understanding of local ferroelectric properties at the nanometer level. One of the most promising approaches is based on scanning probe microscopy (SPM) techniques that allow local property measurements and device characterization on the nanoscale. Among the SPM techniques, the most widely used for ferroelectric imaging currently is piezoresponse force microscopy (PFM).^{1–4} In the last several years, significant attention has been paid to quantitative studies of local ferroelectric behavior by PFM. The early applications include PFM voltage spectroscopy^{5,6} (i.e., measurements of local hysteresis loops at the ~ 10 – 100 nm level). Challenges of quantitative characterization of ferroelectric thin films stem primarily from the inhomogeneous distribution of the tip-generated field and random grain orientation. The problem of relating the PFM signal to the grain orientation was addressed by Harnagea *et al.*,^{7,8} by calculating a full piezoelectric tensor of a ferroelectric sample. In this study, we use a similar approach in conjunction with the local piezoresponse spectroscopy to analyze the effect of grain crystallographic orientation in $\text{SrBi}_2\text{Ta}_2\text{O}_9$ (SBT) ferroelectric thin films on the local switching parameters. The inhomogeneous distribution of the SPM tip-generated field has been taken into account to quantify the piezoresponse signal of individual grains.

The 180-nm-thick SBT films have been prepared by spinning a precursor solution ($\text{Sr}/\text{Bi}/\text{Ta}=0.8/2.2/2.0$) on silicon wafers with $\text{Pt}/\text{TiO}_2/\text{SiO}_2$ buffer layers. Well-shaped macroscopic hysteresis loops have been obtained using Pt top electrodes (Fig. 1). X-ray diffraction analysis indicates that 40% of the volume fraction corresponds to $(hk0)$ oriented grains including 10% of the grains with $(100)/(010)$

orientation, the rest being randomly oriented. The atomic force microscopy and piezoresponse measurements were performed on a commercial instrument (DI Dimension 3000 NS-IIIa) using Au-coated tips.

Comparison of the film surface topography [Fig. 2(a)] with vertical [Fig. 2(b)] and lateral [Fig. 2(c)] PFM images (VPFM and LPFM, respectively) suggests that most grains exist in a single domain state.⁹ Grains that exhibit strong VPFM contrast also have distinctive hysteresis loops [Fig. 3(a)], indicative of large out-of-plane polarization component. For grain 3, the VPFM hysteresis loop is linear, indicative of nonferroelectric nature of the grain or purely in-plane polarization corresponding to (001) orientation.¹⁰ Complementary LPFM hysteresis loops of individual grains are shown in Fig. 3(b). Unlike the vertical PFM hysteresis loops, lateral loops can be oriented in both directions depending on the in-plane polarization orientation with respect to the cantilever axis. This results in higher variability of the LPFM loops.

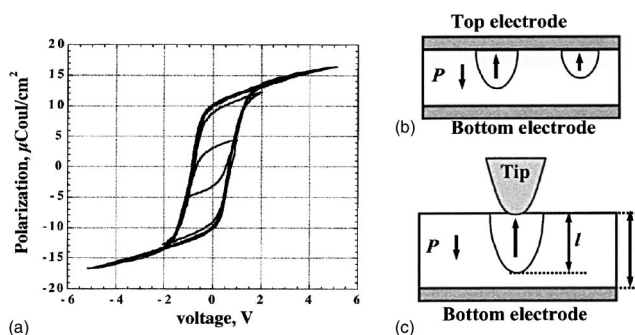


FIG. 1. (a) Polarization hysteresis loops measured in the SBT film using the Pt top electrode. Schematics of the polarization switching process in the macroscopic hysteresis loop measurements (b) and in the PFM experiment (c).

^{a)}Electronic mail: sergei2@ornl.gov

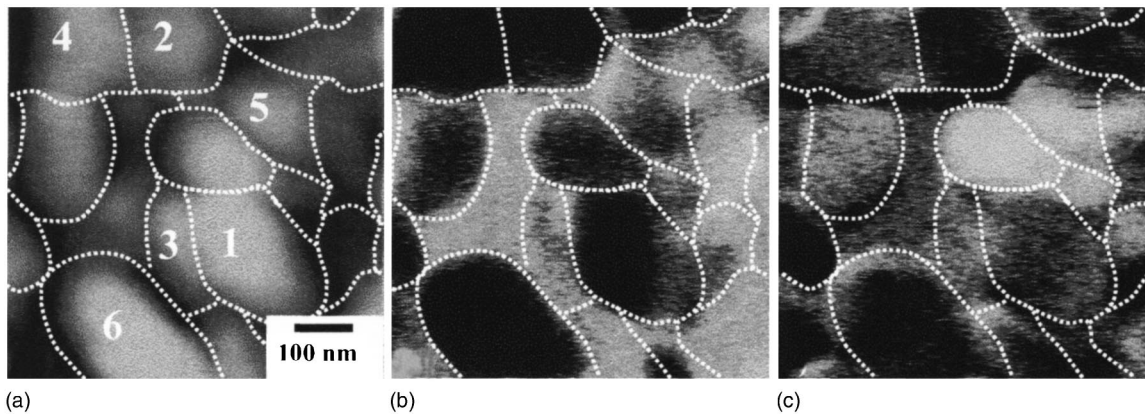


FIG. 2. Surface topography (a), vertical (b), and lateral (c) PFM signal of SBT thin film.

To obtain a deeper insight into the relationship between the grain crystallographic orientation and local spectroscopy, we analyze the shape of the PFM hysteresis loops. Shown in Figs. 1(b) and 1(c) are the schematics of the domain switching process in the macroscopic (plane plate capacitor) and microscopic (PFM) cases. In the macroscopic scenario [Fig. 1(b)], a number of domains nucleate at the electrodes, and the domain size distribution during the growth process determines the hysteresis loop shape. In PFM, the electric field is concentrated directly below the tip, resulting in preferential domain nucleation at the tip-surface junction [Fig. 1(c)]. In thin films, this nascent domain becomes stable when the domain length, l , becomes equal to the film thickness, h , in which case the depolarization energy decreases due to the effective polarization charge compensation by the back electrode. To analyze the hysteresis loop shape in this model, we calculate the vertical surface displacement under the applied tip bias as suggested by Ganpule *et al.*¹¹

$$-\tilde{A}_{\text{piezo}} = \alpha \int_0^{\infty} d_{33} E_z dz = \alpha d_{33} \left\{ \int_0^l E_z dz - \int_l^{\infty} E_z dz \right\}, \quad (1)$$

Integration yields $A_{\text{piezo}} = \alpha d_{33} \{V(0) - 2V(l)\}$, where $V(0)$ is the potential on the surface and $V(l)$ is the potential at the domain boundary. It is shown by Kalinin *et al.*¹² that in the strong indentation regime, for distance l from the center of the contact area larger than contact radius a , the potential distribution inside the material can be approximated using point-charge model. In this case, potential is given as $V(l) = \beta V(0)a/l$, where β is proportionality coefficient. Under typical conditions for PFM loop acquisition, the tip bias is

$V(0) = V_{\text{tip}} = V_{\text{dc}} + V_{\text{ac}} \cos(\omega t)$. Thus, the first harmonic of the tip displacement collected as piezoresponse signal is

$$A_{\text{piezo}} = \alpha d_{33} V_{\text{ac}} \left\{ 1 - 2 \frac{\beta a}{l(V_{\text{dc}})} \right\} \quad (2)$$

Equation (2) describes the late stage (maximum dc bias) of the electromechanical hysteresis loop measured in PFM. It is shown by Molotskii *et al.*,^{13,14} that in the point-charge approximation domain size is related to biasing voltage as $l(V_{\text{dc}}) \sim V_{\text{dc}}$. Hence, the shape of the PFM hysteresis loop for large bias voltages is expected to follow functional form

$$\text{PR} = \alpha d_{33} \{1 - \eta/V_{\text{dc}}\}, \quad (3)$$

where PR is the piezoresponse amplitude, $\text{PR} = A_{\text{piezo}}/V_{\text{ac}}$. To compare the experimental PFM loop shape to Eq. (3), the correction for the capacitive cantilever-surface interaction is introduced by subtracting the linear loop for grain 3 from the hysteresis loops for the ferroelectric grains. A corrected hysteresis loop and corresponding fit by Eq. (3) is shown in Fig. 4(a), illustrating the excellent agreement of the experimental data with the functional form of Eq. (3). The detailed quantitative analysis of domain switching phenomena will be reported elsewhere.¹⁵

To obtain the dependence of the PFM signal and coercive field on grain orientation, we employ the formalism developed by Uchino¹⁶ and later adapted to PFM by Harnagea.⁷ For the SBT sample studied in this work, $d_{33} \approx 19$ pm/V, $d_{32} \approx 1.4$ pm/V, and $d_{31} \approx -1.6$ pm/V.¹⁷ From these values, it is assumed that the crystallographic dependence of PFM response is dominated by the d_{33} value. The longitudinal piezoelectric coefficient measured in the [011] plane at the angle θ from the (010) axis can thus be estimated as $d_{zz}(\theta)$

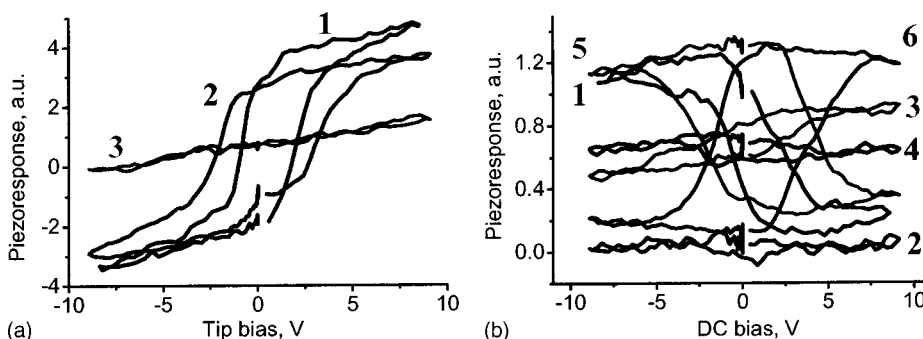


FIG. 3. Vertical (a) and lateral (b) piezoelectric hysteresis loops for grains in Fig. 2. For clarity, vertical loops are shown only for grains 1, 2, and 3.

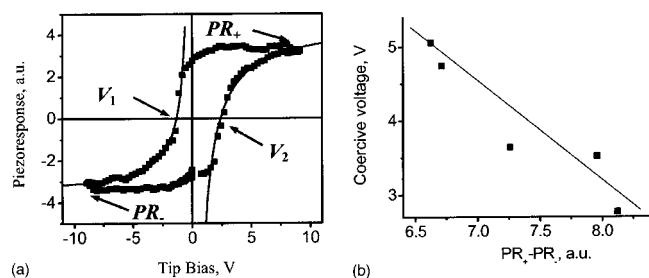


FIG. 4. (a) Corrected hysteresis loop and corresponding fit by Eq. (3) for positive and negative tip biases. (b) Correlation between maximal switchable polarization and coercive voltage V_1+V_2 .

$\approx d_{33} \cos^3 \theta$. Similarly, the lateral piezoresponse coefficient is $d_{zx}(\theta) = d_{31} \cos \theta$. Hence, both vertical and lateral responses decrease with the deviation from (010) orientation. The relationship between the PFM coercive bias and crystallographic orientation of the grain can be estimated from the work of switching, which is proportional to $\mathbf{E} \cdot \mathbf{P} = E P \cos(\theta)$, where \mathbf{E} is electric field and \mathbf{P} polarization vector. Therefore, coercive bias is expected to increase with deviation angle from polar axis as $V_{\text{coer}}(0)/\cos(\theta)$, where $V_{\text{coer}}(0)$ is coercive bias for the (010) grain. Comparison of the angular dependence of piezoresponse signal and coercive bias suggests that for the off-axis orientation of the grains the response decreases and coercive bias increases, in agreement with experimental results illustrated in Fig. 4(b). In the limiting case of the (001)-oriented grain piezoresponse and coercive bias become zero and infinity, respectively. Further quantitative analysis of the switching behavior dependence on grain orientation is hindered by the low symmetry of the SBT material.

To summarize, we have studied the nanoscale switching properties of SBT thin films. Vertical and lateral local hysteresis loops acquired from several single grains demonstrated the significant variability in local switching behavior resulting from different crystallographic orientations. Theoretical description of the vertical hysteresis loop shape is obtained in the point-charge approximation and is shown to be in good agreement with the experimental data. The deviation from ideal (010) orientation results in the decrease of the

PFM signal and increase of the coercive bias in agreement with theoretical expectation.

Research performed in part as a Eugene P. Wigner Fellow and staff member at the Oak Ridge National Laboratory, managed by UT-Battelle, LLC, for the U.S. Department of Energy under Contract No. DE-AC05-00OR22725 (S.V.K.). A.G. acknowledges financial support of the National Science Foundation (Grant No. DMR02-35632). D.A.B. acknowledges financial support from MRSEC Grant No. NSF DMR00-79909. The authors thank K. Hironaka and C. Isobe, Sony Corporation, for providing SBT samples.

¹A. Gruverman, O. Auciello, and H. Tokumoto, *Annu. Rev. Mater. Sci.* **28**, 101 (1998).

²L. M. Eng, S. Grafstrom, Ch. Loppacher, F. Schlaphof, S. Trogisch, A. Roelofs, and R. Waser, *Adv. Solid State Phys.* **41**, 287 (2001).

³*Nanoscale Characterization of Ferroelectric Materials*, edited by M. Alexe and A. Gruverman (Springer, Berlin), 2004.

⁴*Nanoscale Phenomena in Ferroelectric Thin Films*, edited by S. Hong (Kluwer Academic, Boston, 2004).

⁵M. Alexe, A. Gruverman, C. Harnagea, N. D. Zakharov, A. Pignolet, D. Hesse, and J. F. Scott, *Appl. Phys. Lett.* **75**, 1158 (1999).

⁶A. Roelofs, U. Boettger, R. Waser, F. Schlaphof, S. Trogisch, and L. M. Eng, *Appl. Phys. Lett.* **77**, 3444 (2000).

⁷C. Harnagea, A. Pignolet, M. Alexe, and D. Hesse, *Integr. Ferroelectr.* **38**, 23 (2001).

⁸C. Harnagea, Ph.D. thesis, Martin-Luther-Universität Halle Wittenberg, Halle, 2001.

⁹Shown here are PFM images representing the $A \cos \theta$ signal, where A is piezoresponse amplitude and θ is phase.

¹⁰A. Gruverman, A. Pignolet, K. M. Satyalakshmi, M. Alexe, N. D. Zakharov, and D. Hesse, *Appl. Phys. Lett.* **76**, 106 (2000).

¹¹C. S. Ganpule, V. Nagarjan, H. Li, A. S. Ogale, D. E. Steinhauer, S. Aggarwal, E. Williams, R. Ramesh, and P. De Wolf, *Appl. Phys. Lett.* **77**, 292 (2000).

¹²S. V. Kalinin, E. Karapetian, and M. Kachanov (unpublished).

¹³M. Molotskii, *J. Appl. Phys.* **93**, 6234 (2003).

¹⁴M. Molotskii, A. Agronin, P. Urenski, M. Shvebelman, G. Rosenman, and Y. Rosenwaks, *Phys. Rev. Lett.* **90**, 107601 (2003).

¹⁵S. V. Kalinin, A. Gruverman, E. Karapetian, M. Kachanov, J. Shin, and A. P. Baddorf (unpublished).

¹⁶X. Du, U. Belegundu, and K. Uchino, *Jpn. J. Appl. Phys., Part 1* **36**, 5580 (1997).

¹⁷X. L. Lu and D. A. Payne, presented at the Electroceramics 2000 Conference, Portoroz, Slovenia.